Analysis of the Zeeman effect on D_α spectra on the EAST tokamak*

Wei Gao(高伟)†, Juan Huang(黄娟)‡, Chengrui Wu(吴承瑞), Zong Xu(许棕), Yumei Hou(侯玉梅), Zhao Jin(金钊), Yingjie Chen(陈颖杰), Pengfei Zhang(张鹏飞), Ling Zhang(张凌), Zhenwei Wu(吴振伟), and EAST Team

Institute of Plasma Physics, Chinese Academy of Sciences, Hefei 230031, *China*

(Received 28 November 2016; revised manuscript received 17 January 2017; published online 20 February 2017)

Based on the passive spectroscopy, the D_α atomic emission spectra in the boundary region of the plasma have been measured by a high resolution optical spectroscopic multichannel analysis (OSMA) system in EAST tokamak. The Zeeman splitting of the D_α spectral lines has been observed. A fitting procedure by using a nonlinear least squares method was applied to fit and analyze all polarization π and $\pm\sigma$ components of the D_α atomic spectra to acquire the information of the local plasma. The spectral line shape was investigated according to emission spectra from different regions (e.g., low-field side and high-field side) along the viewing chords. Each polarization component was fitted and classified into three energy categories (the cold, warm, and hot components) based on different atomic production processes, in consistent with the transition energy distribution by calculating the gradient of the D_α spectral profile. The emission position, magnetic field intensity, and flow velocity of a deuterium atom were also discussed in the context.

Keywords: Zeeman effect, plasma, spectrum, deuterium

PACS: 52.70.Kz **DOI:** 10.1088/1674-1056/26/4/045203

1. Introduction

The edge plasma performance determines the level of impurities in the core plasma and influences the core plasma confinement, which plays a critical role in the fusion plasma.[1–3] Since the electron temperature and density decrease rapidly beside the scrape-off layer, the recycling processes are affected and dominated by atom and molecular processes in the boundary region of the plasma.[4] Therefore, it is important to study atomic and molecular spectra in the boundary region. Based on high resolution spectroscopy, the line shape of the spectra was studied and used to acquire more information of the local plasma. The magnetic field can affect the atomic and molecular spectral shape, which is called the Zeeman effect. The Zeeman effect can be fully understood by quantum mechanics, and it has been investigated in many ways on different fusion plasma.[5–19] On TEXTOR,[5–8] the emission spectra with the Zeeman effect had been studied, and Zeeman spectroscopy have been introduced as a tool for studying atomic processes in edge plasma. The Zeeman effect in hydrogen-like systems and its influence on fusion plasma temperature measurement have been studied in detail on JET.[9,10] On Alcator C-Mod,[11–13] the neutral atom temperature and flow measurement by Zeeman split spectra was introduced. The D_α spectra of the Zeeman effect with all polarization components (π and $\pm\sigma$ components) were analyzed from one emission region (inner divertor region) and the viewing angle θ was considered. On TRIAM-1M,[14–17] the local values of the magnetic field strength, population density, temperature, and flow velocity by analyzing the Zeeman split spectra of H_α, He I and the H_2 Fulcher-α band have been evaluated. By observing the polarization $\pm\sigma$ components of the spectra, the viewing angle θ did not need to be considered.[14,15,17] The hydrogen emission spectra in the boundary region were considered from two different emission regions (high-field $B_{\rm in}$ and low-field $B_{\rm out}$) and roughly classified into two[14] or three[15,17] categories. On LHD,[18,19] the Zeeman split spectra of He I was used to determine the local values of the magnetic field strength and the emission position near the ergodic layer[18] and the theoretical works about the Zeeman effect of the spectra were introduced.[19] According to previous studies, the spectra were considered separately in different regions for a gradient magnetic field along the viewing chord, and emission position, magnetic field intensity, and flow velocity could be acquired by analyzing the Zeeman patterns of the spectra.

In this paper, the spectral line-shape method based on high resolution spectra was used to analyze the D_α atomic emission spectra of all polarization π and $\pm\sigma$ components to acquire the important and useful parameters of the local plasma. For the effect of the instrument function of the optical spectrometer system, it was considered in data analysis. A fitting procedure using the nonlinear least squares method

*Project supported by the National Natural Science Foundation of China (Grant Nos. 11275231 and 11575249) and the National Magnetic Confinement Fusion Energy Research Program of China (Grant No. 2015GB110005).

†Corresponding author. E-mail: gaowei@ipp.ac.cn

‡Corresponding author. E-mail: juan.huang@ipp.ac.cn

© 2017 Chinese Physical Society and IOP Publishing Ltd

was applied to fit and analyze the D_α atomic spectra to acquire the information of the local plasma. The emission position, magnetic field intensity, and flow velocity of a deuterium atom were determined and the transition energy distribution of the atom was simulated. For more accurate and credible analyses, the hot components and their wavelength drifts in different regions were considered separately, and the intensity of $\pm\sigma$ components with $I_{+\sigma} \neq I_{-\sigma}$ was also discussed.

The paper is organized as follows. The experimental setup and diagnostic performance are introduced in Section 2. The theory of the Zeeman effect and the basic principles of the fitting procedure are given in Section 3. Detailed discussion and analysis of the D_α atomic emission spectra are discussed in Section 4. Finally, Section 5 summarizes our results.

2. Experimental setup and diagnostic performance

The EAST is a medium-sized magnetic fusion device, which uses the superconducting coils to create a spiralling magnetic field configuration with an ITER-like D-shaped cross section. It has a major radius of about 1.85 m and minor radius of about 0.45 m with the toroidal magnetic field currently operated in range of $B_t = 1.2$ T$\sim$ 3.5 T. It has a flexible PF control system with separate power supply for each PF coil to accommodate both double null (DN) and upper/lower single null (USN/LSN) divertor configurations. The lower and upper divertors are covered by graphite tiles. In a recent upgrade, the upper graphite divertor has been replaced with an ITER-like tungsten monoblock divertor.

A high resolution optical spectroscopic multichannel analysis (OSMA) system was used to observe atom emissions in the boundary region in EAST. The schematic diagram of the experiment is shown in Fig. 1. Two arrays of 13 viewing chords, with a spot diameter about 2.2 cm, the angle between the adjacent about 2° and the spatial resolution less than 5.5 cm near the divertor target, were used to observe the atomic emission spectra in the lower and upper divertor regions. The OSMA system is equipped with an SP750 spectrometer and ProEM EMCCD 1024B camera. The spectrometer has a focal length of 750 mm and features a triple indexable gratings (2400 g/m@600 nm, 1200 g/m@500 nm, 1200 g/m@300 nm) and triple grating turret, which includes a direct digital grating scan mechanism with full wavelength scanning capabilities. The detector is a back-illuminated, thermoelectrically cooled 1024×1024 pixels with the size of 13 μm ×13 μm, and has a dynamic range of 16 bits. The electron–multiplying charge coupled device (EMCCD) has the advantage of high sensitivity, extremely low etaloning, baseline-active stability engine, EM and non-EM modes for the lowest noise and the best linearity. In the experiment, D_α atomic spectra were observed in the lower divertor region. The detector was typically operated at 5 $\sim$ 20 frames/s for different conditions of plasma. For acquiring the high spectral resolution, the 2400-g/m grating was used to observe the D_α spectra (656.1 nm) to study the Zeeman effect, and the width of slit was adjusted to 10 μm. The detector array was binned into 13 channels of 60 rows each and the exposure time was set from 40 ms to 90 ms to decrease the readout time and increase the signal-to-noise ratio. The reciprocal linear dispersion is 0.286 nm/mm at 656 nm, and the wavelength resolution is 0.013 nm at full width at half maximum (FWHM). The instrument function for channel 8 of the OSMA system is 0.0105 nm. In the present work, the analyzed discharges were conducted in single null divertor configuration, and the plasma was sustained by 4.6-GHz lower hybrid current drive (LHCD). During the LHCD phase, the plasma current $I_p \sim 450$ kA, the core electron temperature $T_e \sim 1.2$ keV and line-averaged electron density $n_e \sim 3.8 \times 10^{19}$ m^{-3}.

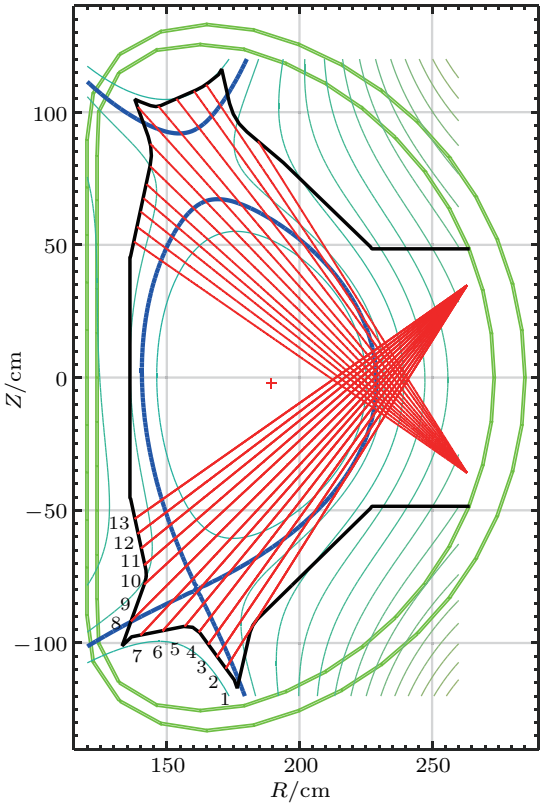


Fig. 1. (color online) Schematic diagram of the EAST poloidal section with viewing lines for OSMA system.

3. Analysis method for Zeeman effect

According to the quantum mechanical interaction between an atom and an external electromagnetic field ($\boldsymbol{B}$), in first order perturbation theory, the change in energy due to the perturbation could be expressed as[20,21]

$$H' = H_{so} + H_{magn}. \tag{1}$$

Here, the relative strength between the spin–orbit interaction and the external magnetic field affection should be considered.

When the spin–orbit interaction is dominant, it belongs to the weak field effect, and in contrast, it belongs to the strong field effect. The criterion for judging the weak and strong field effects can be expressed as:

$$\begin{cases} \text{strong field effect: } B \gg \dfrac{Z^4}{n^3 l(l+1)} \cdot 12.5, \\ \text{weak field effect : } B \gg \dfrac{Z^4}{n^3 l(l+1)} \cdot 12.5. \end{cases} \tag{2}$$

From the above criterion, the strong field effect is dominant for D_α spectra in EAST. Therefore, the perturbation of the energies could be simplified from Eq. (1) as:

$$\Delta E_{\text{magn}} = \mu_{\text{B}} g B m_j, \tag{3}$$

where μ_{B} is Bohr magneton,

$$g \equiv 1 + \frac{j(j+1)+s(s+1)-l(l+1)}{2j(j+1)}$$

is the Landé factor. The magnitude of the local magnetic field affects the magnitude of the wavelength shift of the Zeeman components of the spectral lines. The wavelength shift of the Zeeman components $\delta\lambda_z$ is approximately equal to $\delta\lambda_z = \lambda_0^2 kB$, where λ_0 is the central wavelength of the unshifted line and $k = 0.46686\ \text{cm}^{-1}/\text{T}$.

Based on Wigner–Eckart theorem,[22] the transition intensity I between the upper and lower states can be expressed as:

$$I^q_{n'l'm'nlm} = (-1)^{l_>-m'} \sqrt{l_>} \begin{pmatrix} l & 1 & l' \\ m & q & -m' \end{pmatrix} \Re, \tag{4}$$

where $l' = l+1$, $q = m'-m$, defining $l_> \equiv \max(l', l)$, and $\Re \equiv \int_0^\infty R_{n'l'} r^3 R_{nl}\, \mathrm{d}r$, R_{nl} is the radial part of the hydrogenic wavefunction. By studying the polarization of the emitted radiation, the unshifted component (π) is parallel to the magnetic field and the shifted components ($\pm\sigma$) are perpendicular to the magnetic field, of which the ratio is governed by the viewing angle (θ) between the magnetic field and the view chord. At any given observation angle θ, and in the absence of an additional polarization effect, the intensity ratio of the π and $\pm\sigma$ components is approximately equal to $I_\pi : I_{\pm\sigma} = \sin^2\theta : \frac{1}{2}(1+\cos^2\theta)$. In fact, it can no longer assume that $I_{+\sigma} = I_{-\sigma}$ in the plasma spectrum,[12] because it is valid for the individual Zeeman components. The asymmetry of the σ components is possibly explained by the relationships among l, temperature, viewing angle (θ) and the magnetic field B,[12] but the particular data processing method was not introduced and done. Here, according to the quantum mechanicals of the Zeeman effect by Eq. (4), the $+\sigma$ and $-\sigma$ components were considered as a whole in this work and the intensity ratio of the π and all σ components can be approximately expressed as $I_\pi : (I_{-\sigma} + I_{+\sigma}) = \sin^2\theta : (1+\cos^2\theta)$, so the asymmetry of σ components can be solved. At the same time, the spectra of deuterium atoms in the boundary region were considered as a separated spectrum from the low field and the high field, and roughly classified into three energy categories based on different atomic production processes: the cold (0 eV–1 eV, recombination and dissociation), warm (1 eV–10 eV, dissociation), and hot (> 10 eV, charge exchange and surface reflection).[14–17,22,23]

4. Discussion

4.1. Fitting of D_α spectra

The D_α emission spectra ($2^2P_{1/2,3/2}$–$3^2D_{3/2,5/}2$, $2^2S_{1/2}$–$3^2P_{1/2,3/2}$, $2^2P_{1/2,3/2}$–$3^2S_{1/2}$: 656.1 nm) in the lower divertor region were observed in the 4.6-GHz LHCD plasma, the toroidal magnetic field strength B_0 was -2.48 T at the major radius of $R_0 = 1.85$ m (magnetic axis), plasma current was 450 kA, the core electron temperature T_e was 1.2 keV and the line-averaged electron density was 3.8×10^{19} m^{-3}. In this paper, the basic elements in the fitting procedure used in previous works[13–15,17] were integrated into the new fitting procedure. Here, the hot components and their wavelength drifts of different polarization components of the spectra (π and $\pm\sigma$ components) from different regions (low field and high field) should be considered separately,[23,24] so six hot components and their wavelength drifts were considered in the present work. In this paper, the mainly important factors considered in our fitting procedure includes all polarization components of the spectra (π and $\pm\sigma$ components), the viewing angle θ, the intensity ratio of the π and all σ components, two different emission regions (high-field and low-field), and three different categories (the cold, warm, and hot components) and their wavelength drifts of spectra for each emission region.

In the present work, the measured spectra of the Zeeman effect are mainly broadened by the following essential elements: the first is the Doppler broadening of the observed spectra, the second is caused by the instrument function, the third is the Zeeman split, and the last is Stark broadening. Compared with other broadening factors, the Stark broadening $\Delta\gamma_{\text{Stark}}$ (about 0.001 nm at the boundary region) is too small and can be ignored. In general, both of these elements are a Gaussian lineshape, and the resultant convolution is still a Gaussian lineshape which could be expressed as:

$$F(\lambda) = y_0 + \sum_{k=1}^{N}\sum_{j=1}^{3} a_j w_j A_k W_k \sqrt{\frac{\pi}{4\ln 2(w_j^2+W_k^2)}} \times \exp\left[-4\ln 2\frac{(\lambda-\lambda_k)^2}{(w_j^2+W_k^2)}\right]. \tag{5}$$

Here, $F(\lambda)$ is the final equation of two Gaussian lineshape convolution, y_0 is the background level, a_j and w_j are the amplitude and FWHM of the instrument function, A_k, λ_k, and W_k are the amplitude, center wavelength, and FWHM of spectra

line k. Here, the instrument function was measured by He–Ne laser lamp. A nonlinear least squares method was used to fit the D_α spectra. In this work, the wavelength of the observed spectra is lacking an absolute wavelength reference and the value is calculated by the program of the OSMA system. Therefore, the flow velocity in this paper is the relative flow velocity, which is calculated by the Doppler shift between the high field and low field. The red circles shown in Fig. 2(a) are measured spectra by OSMA subtracted background (e.g., bremsstrahlung, dark noise), along the viewing chord (channel 8 in Fig. 1) at $t = 4.12$ s plasma discharge. The line shown in Fig. 2(a) is corresponding to the calculated one according to different energy components, considering the instrumental broadening, the Doppler broadening, and the Zeeman effect, with the residuals shown in Fig. 2(b). Each calculated spectral line from high field ($B_{\rm in} = 3.2$ T) and low field ($B_{\rm out} = 1.9$ T) is shown in panels (c) and (d), respectively. The viewing angle θ between the magnetic field and the view chord is calculated as 71.78°. From Fig. 1, by comparison of the emission spectra in the high field and the low field, we conclude that the emission spectra in the high field is the dominant component of the line-average emission spectra, and this conclusion is similar to the hypothesis in the previous work[13] in which they assumed that the emission spectra were only from the inner divertor region. For the pink shadow area in Fig. 2(a), the left part of the spectrum (wavelength less than 656.1420 nm) can be assumed to be composed of the $+\sigma$ component of the emission spectra in the high field; this part of the spectra will be discussed in Subsubsection 4.2.2.

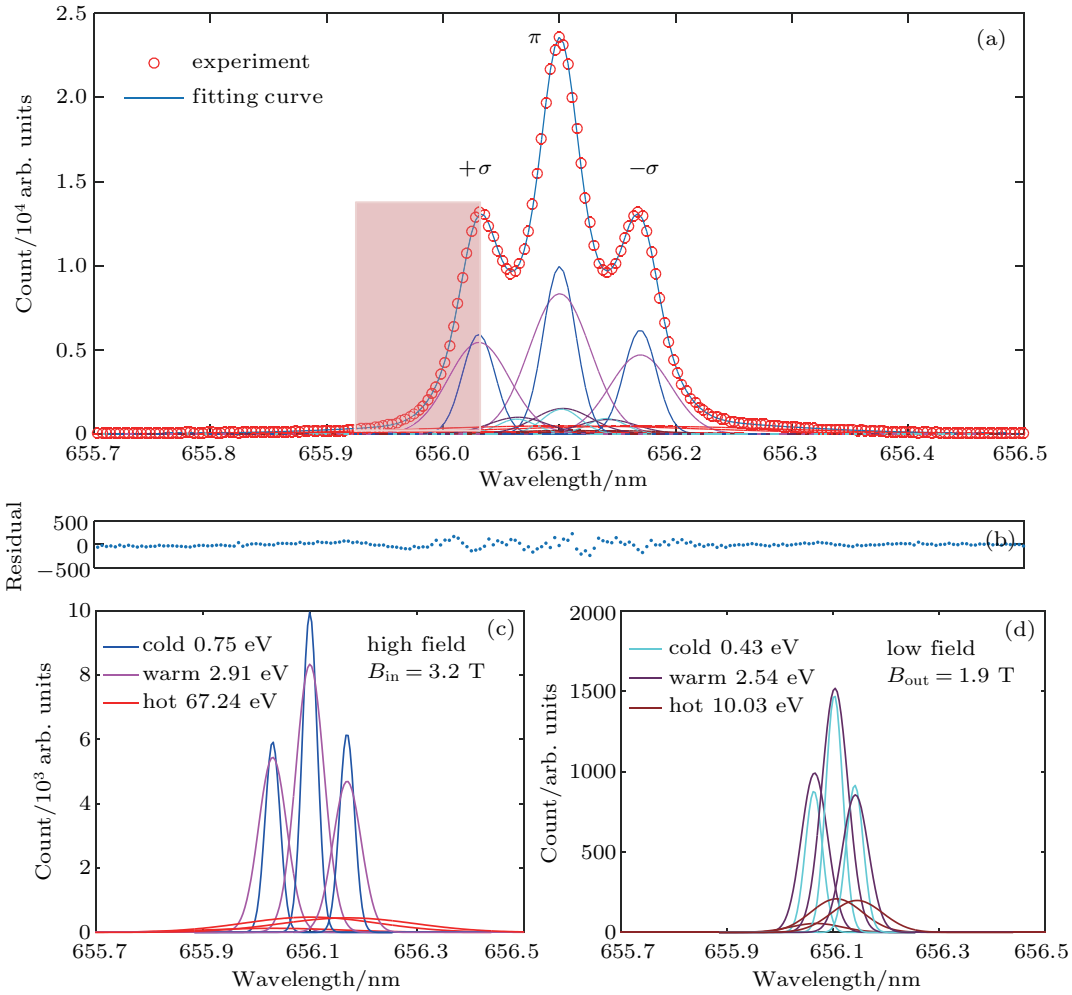


Fig. 2. (color online) (a) The open red circles corresponding to the D_α measurement from channel 8 viewing chord subtracting background (e.g., bremsstrahlung), and the line representing the calculated one without considering bremsstrahlung emission; (b) the fitting data residuals; each calculated line corresponding to three components in the high field (c) and the low field (d).

4.2. Flow velocity measurements and the relative energy distribution of particles

4.2.1. Flow velocity measurements

For lack of an absolute wavelength reference, the relative flow velocity of the cold component of deuterium atoms is estimated based on the relative Doppler shifts of the separated spectra in the low field and the high field. The spatial profile and the time-variant of the measured flow velocities of deuterium atom cold components as projections on the viewing chords and times are shown in Figs. 3(a) and 3(b), respectively. The error bar shown with the filled circles is the standard deviation of the fitting procedure in Fig. 3. From Fig. 3,

the relative flow velocity of the cold component (channel 8) is estimated at about 3.8 km/s. The possible models for flow in the edge, which are flow reversal, edge toroidal rotation emanating from the core, and $\boldsymbol{E}\times\boldsymbol{B}$ poloidal drifts, could be used to explain from the aspects of the magnetic field in diverted discharge, the inward radial atomic pressure gradient flow and outward friction force.[11] In diverted discharge, the helicity of the magnetic field causes motion along the field line to have strongly correlated toriodal and polodial components. The toroidal flow observed near the high field is counterclockwise, while that observed near the low field is opposite, which to an observer in the inner and outer divertor is a downward, poloidal motion. For the flow in the outer SOL, the counterclockwise toroidal flow implies a clockwise poloidal flow, again a downward motion in the outer divertor. The toroidal and poloidal flows are driven by the ion–atom friction force along the magnetic field and in the direction of cross-field ion drifts, respectively, in which the momentum is transferred by charge-exchange and elastic collisions. The radial flow is driven by the inward radial atomic pressure gradient and outward friction force is due to the diffusion of ions.

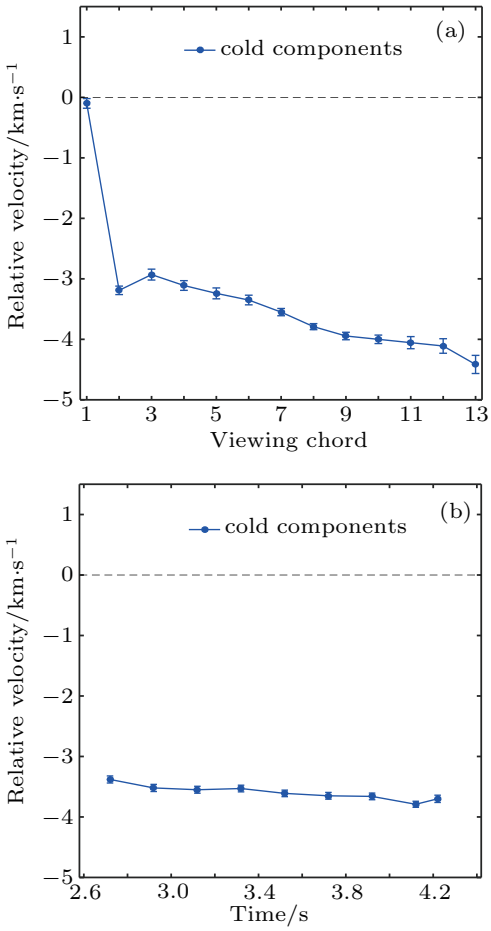


Fig. 3. (color online) The spatial profile of the flow velocity of cold temperature components as projections on the viewing chords is shown at 4.12 s in panel (a). The time-variant of the flow velocity of the cold component of channel 8 is shown in panel (b). The error bar with the filled circles is also given.

4.2.2. The relative transition energy distribution of particles

Since the line shape can be acquired by fitting procedure, the translation energy distribution of the excited atom can be obtained through an analysis of the line shape of its emission spectrum. The translation energy distribution $f(E(\Delta\lambda))$ is proportional to $\mathrm{d}I(\Delta\lambda)/\mathrm{d}\lambda$.[23,24] In the present work, although the different components of the emission spectra were blended and not easy to distinguish, the line shape obtained by the fitting procedure can be used to simulate the translation energy distribution. According to the above analyses of the relative Doppler effect of the deuterium ($n=3$) atom emission spectra in Subsection 4.1, the line shape of the different temperature components can be acquired and used to simulate the relative translation energy distribution of D_α spectra from the high field and the low field by the relative wavelength center in Fig. 4. It shows that the three-temperature component distribution of the π component in the high field is different from that in the low field. For the cold component (0 eV–1 eV, recombination and dissociation), the peak value of the translation energy distribution (0.13 eV) in the high field is greater than that (0.08 eV) in the low field. It is possibly due to the higher atomic energy in the high field than that in the low field. For the warm part (1 eV–10 eV, dissociation), and the hot part (>10 eV, charge exchange and surface reflection), the distribution of those two temperature components in the high field is also wider and greater than that in the low field. It can be explained by the different plasma conditions between the high field and the low field. It is also shown that the spectra should be considered separately. In Subsection 4.1, according to the fitting result, the emission spectra in the high field is dominant, so the pink shadow area of the spectrum (wavelength less than 656.1420 nm) in Fig. 2(a) can be considered only from the high field. Here this part of the spectra is used to calculate the gradient and to compare with the simulated translation energy distribution, which shows that they have the similar distribution and a good agreement.

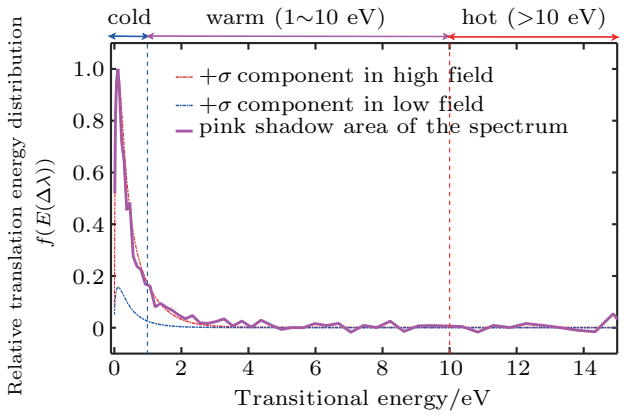


Fig. 4. (color online) The relative transition energy distribution of deuterium ($n=3$) emission spectra from the high field and low field are simulated. The gradient of the pink shadow area of the spectrum in Fig. 2(a) (wavelength less than 656.1420 nm) is done to compare with the simulated results.

4.3. Estimation of the position of emission

In EAST tokamak, the total magnetic field $B_{\rm tot}$ is made up of two components, a toroidal field $B_{\rm t}$ and a poloidal field $B_{\rm p}$. Magnetic field data for EAST discharges are based on a combination of measurements and reconstructions. The toroidal field $B_{\rm t}(R)$ could be calculated as $B_{\rm t}(R) = B_0R_0/R$, where $B_0 = -2.48$ T is the magnetic field measured at major radius of $R_0 = 1.85$ m (magnetic axis). The poloidal field $B_{\rm p}$ could be calculated by $B_{\rm R}$ and B_Z components which are taken from the EFIT code. The total magnetic field is shown in Fig. 5.

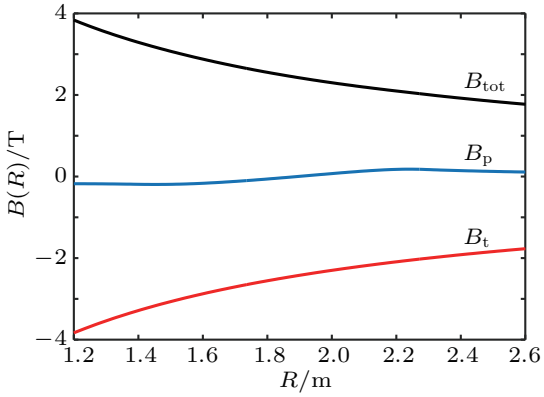


Fig. 5. (color online) The magnitude of the magnetic fields at EAST plotted against the major radius R. The two bottom curves are the toroidal and poloidal fields, and the top curve is the total field $B_{\rm tot} = \sqrt{B_{\rm p}^2 + B_{\rm t}^2}$.

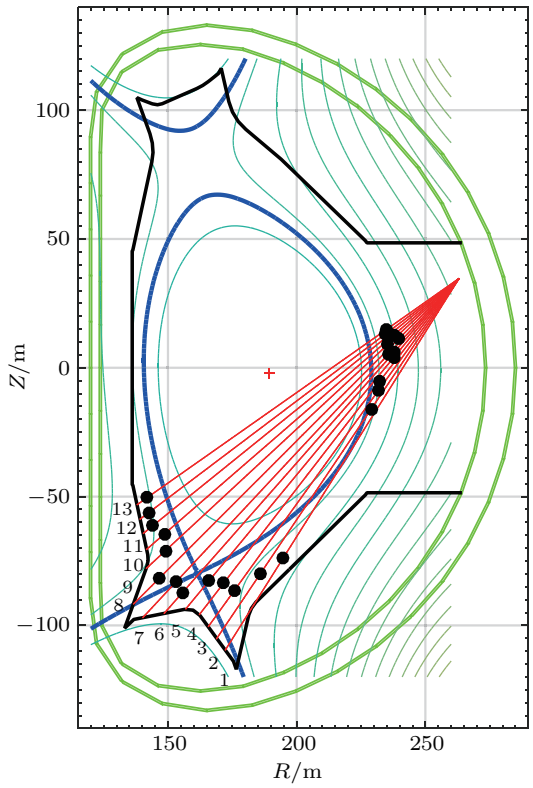


Fig. 6. (color online) Schematic drawing of the EAST showing the location of the last closed magnetic flux surface (blue line) and the separated position of the D_α emission (filled circles).

In the fitting procedure, the magnetic field effect at low field and high field is considered separately, which means the D_α emission spectra consist of emission spectra from two different regions (high-field $B_{\rm in}$ and low-field $B_{\rm out}$). In Fig. 2, the magnetic field can be acquired by fitting the measured spectra to achieve the Zeeman split of the spectra and the magnetic field intensity in the low field and high field are 1.9 T and 3.2 T, respectively. By comparison with Fig. 5, the emission spectra locations can be acquired. The separated D_α emission positions of all viewing chords are shown in Fig. 6 and the filled circles along all viewing chords indicate the separated positions of deuterium atom emission spectra at the present condition of plasma. The blue line shows the position of the last closed flux surface (LCFS).

5. Conclusion

In diverted configuration, the D_α emission spectra from the divertor region were measured in EAST tokamak. The Zeeman effect on observed spectra with all polarization π and $\pm\sigma$ components was studied and applied to acquire the local plasma information about the relative flow velocity, magnetic intensity, emission position, and the relative transition energy distribution of particles. A new fitting procedure was applied and discussed in detail. The relative Doppler shift of the separated spectra was used to determine the relative flow velocity, and the Zeeman split of the spectra was used to acquire the magnetic field intensity and emission position. By the line shape obtained from the fitting procedure, the relative transition energy distribution of particles can be simulated and compared with the gradient of part of the measured spectra. In this paper, the spectroscopy by using the Zeeman effect is used to measure the neutral dynamics and acquire the important information of the neutral atoms in the boundary region of plasma. In the future, this technique will be extended to the observation of the Fulcher-α band and hydrogen-like systems (i.e., He II $n = 3$–4 transition at 468.7 nm) spectra in EAST.

References

[1] Neuhauser J, Schneider W, Wunderlich R and Lackner K 1984 *Nucl. Fusion* **24** 39
[2] Stangeby P C and McCracken G M 1990 *Nucl. Fusion* **30** 1225
[3] Groebner R J 1993 *Phys. Fluids B* **5** 2343
[4] Monk R, Loarte A, Chankin A, Clement S, Davies S J, Ehrenberg J K, Guo H Y, Lingertat J, Matthews G F, Stamp M F and Stangeby P C 1997 *J. Nucl. Mater.* **241–243** 396
[5] Hey J D, Lie Y T, Rusbüldt D and Hintz E 1994 *Contrib. Plasma Phys.* **6** 725
[6] Hey J D, Korten M, Lie Y T, Pospieszczyk A, Rusbüldt D, Schweer B, Unterberg B, Wienbeck J and Hintz E 1996 *Contrib. Plasma Phys.* **5** 583
[7] Hey J D, Chu C C and Mertens Ph 2002 *Contrib. Plasma Phys.* **42** 635
[8] Hey J D, Chu C C and Mertens Ph 2002 *Phys. Plasmas* **645** 26
[9] Blom A and Jupén C 2002 *Plasma Phys. Control. Fusion* **44** 1229
[10] Carolan P, Forrest M, Peacock N and Trotman D 1985 *JETP* **85** 05
[11] Benjamin R, Terry J and Moos H 1988 *Phys. Rev. A* **37** 537

[12] Weaver J L, Welch B L, Griem H R, Terry J, Lipschultz B, Pitcher C S, Wolfe S, Pappas D A and Boswell C 2000 *Rev. Sci. Instrum.* **71** 1664

[13] Welch B L, Weaver J L, Griem H R, Noonan W A, Terry J, Lipschultz B and Pitcher C S 2001 *Phys. Plasmas* **8** 1253

[14] Shikama T, Kado S, Zushi H and Tanaka S 2004 *Phys. Plasmas* **11** 4701

[15] Shikama T, Kado S, Zushi H, Sakamoto M and Iwamae A 2006 *Plasma Phys. Control. Fusion* **48** 1125

[16] Shikama T, Kado S and Tanaka S 2007 *Phys. Plasmas* **14** 072509

[17] Shikama T, Fujii K, Kado s, Zushi H, Sakamoto M, Iwamae A, Goto M, Morita S and Hasuo M 2011 *Can. J. Phys.* **89** 495

[18] Goto M and Morita S 2002 *Phys. Rev. E* **65** 026401

[19] Shikama T, Fujii K, Mizushiri K, Hasuo M, Kado s and Zushi H 2009 *Plasma Phys. Control. Fusion* **51** 122001

[20] Bethe H A and Salpeter E E 1957 *Quantum Mechanics of one-and two-electron atoms* (Berlin: Springer-Verlag)

[21] Bransden B and Joachain C 1983 *Physics of Atoms and Molecules* (New York: Longman Scientific & Technical Publishers)

[22] Cowan R D 1981 *The Theory of Atomic Structure and Spectra* (Berkely: University California Press)

[23] Xu W, Wan B N, Zhou Q, Wu Z W, Mao J S and Li J G 2004 *Chin. Phys.* **13** 1510

[24] Ogawa T and Higo M 1979 *Chem. Phys. Lett.* **65** 610